Triple-Helix Formation by an Oligonucleotide Containing One $(dA)_{12}$ and Two $(dT)_{12}$ Sequences Bridged by Two Hexaethylene Glycol Chains

M. Durand, S. Peloille, N. T. Thuong, and J. C. Maurizot*

Centre de Biophysique Moléculaire, 1A, Avenue de la Recherche Scientifique, 45071 Orléans Cedex, France

Received March 19, 1992; Revised Manuscript Received June 30, 1992

ABSTRACT: The triple-helix formation by the oligonucleotide $(dA)_{12}$-x-$(dT)_{12}$-x-$(dT)_{12}$, where x is a hexaethylene glycol group, was investigated by thermal denaturation analysis and circular dichroism spectroscopy. Thermal denaturation analysis showed that this single-stranded oligonucleotide is able to fold back on itself twice to give a triple helix at low temperature. Upon an increase in the temperature, two cooperative transitions were observed: formation of a double-stranded structure with a dangling x-$(dT)_{12}$ extremity, then formation of a single-stranded coil structure. Due to the intramolecular character of the transition, the triplex is much more stable than that formed by the reference mixture $(dA)_{12}$ + $2(dT)_{12}$. In 0.1 M NaCl, the triplex-to-coil transition occurred at about 30 °C whereas the duplex-to-coil was at about 60 °C. Upon an increase in the salt, the increase of temperature corresponding to the triplex-to-duplex transition was larger than that of the duplex-to-coil transition. $MgCl_2$ showed higher efficiency than NaCl to promote triplex or duplex formation. The thermodynamic parameters ΔH and ΔS were determined at various ionic strengths for both transitions. Both the enthalpy change and entropy change associated with triplex-to-duplex transition (Hoogsteen base pairing) were smaller than those associated to the duplex-to-coil transition (Watson–Crick base pairing). When the ionic strength increased, the parameters $-\Delta H$ and $-\Delta S$ showed a very small decrease for the duplex-to-coil transition whereas a strong increase was observed with the triplex-to-duplex transition. A total of 3.5 ± 0.3 sodium ions are thermodynamically released in the triplex-to-duplex transition, whereas this number is 2.3 ± 0.3 in the duplex-to-coil transition. CD spectroscopy demonstrated that the conformation of the triplex structure of $(dA)_{12}$-x-$(dT)_{12}$-x-$(dT)_{12}$ was essentially identical to that of the reference mixture $(dA)_{12}$ + $2(dT)_{12}$. These results open up new prospects for the use of this type of oligonucleotide in studies of triple helix properties.

The existence of triple-stranded structures formed by synthetic homopurine–homopyrimidine sequences was reported several decades ago (Felsenfeld et al., 1957; Riley et al., 1966; Michelson et al., 1967; Morgan & Wells, 1968). These studies, together with more recent ones, have identified the sequence requirements and the ionic strength and pH conditions for the formation of RNA or DNA triplexes (Marck & Thiele, 1978; Douglas et al., 1979; Lee et al., 1987; Antao et al. 1988). Triplex DNA has generally been formulated as major-groove binding of polypyrimidines in parallel orientation to a polypurine segment within duplex DNA by Hoogsteen base pairing. Over the past few years, the interest in the triple-helical structure in DNA has been renewed. First, there was evidence of the presence of intramolecular triple helices (H-form of DNA) in biological systems (Lyamichev et al., 1986; Mirkin et al., 1987; Lee et al., 1987; Voloshin et al., 1988), and some suggestions that pyr-pur-pyr DNA stretches might have a biological role, particularly in gene regulation, were advanced (Kohwi et al., 1988; Htun & Dahlberg, 1988; Johnson, 1988; Hanvey et al., 1988; Wells et al., 1988). Second, more recently, potential for therapeutic applications in which gene expression is repressed by triplex formation was explored (Moser & Dervan, 1987; Le Doan et al., 1987; Strobel et al., 1988; Praseuth et al., 1988; Cooney et al., 1988; Francois et al., 1988, 1989; Posvic & Dervan, 1989; Perrouault et al., 1990). So, it has been shown that short oligodeoxynucleotides are able to bind to double-stranded DNA with high sequence specificity, a novel function that is 10^6 times more specific than restriction enzymes (Moser & Dervan, 1987; Le doan et al., 1987; Lyamichev et al., 1988; Federova et al., 1988).

All these studies, even if the biological function of the triple-stranded DNA is not yet clear, make the investigation of the physical properties of the triple-stranded DNA necessary. This has been helped by the emergence, in the 1980s, of automated DNA synthesizers and the advent of 2D NMR spectroscopy which made an in-depth study of the triple helices possible. NMR studies of short triplexes have been reported on both octamer (Rajagopal & Feigon, 1989a,b) and 11-mer (Santos et al., 1989) triplexes containing both T·A·T and C·G·C^+ base triplets and stabilized by low pH and/or $MgCl_2$. More recently, experiments probing the formation of stable short DNA triplexes containing only T·A·T base triplets have been reported (Pilch et al., 1990a,b; Umemoto et al., 1990; Kibler-Herzog et al., 1990). One difficulty encountered in these studies is caused by the low stability of the complex formed which makes the use of a high concentration of oligonucleotide and/or the high concentration of NaCl, $MgCl_2$, spermine, etc. necessary. One possibility to overcome this problem is to use an oligonucleotide with a sequence such that it can fold back on itself to form a triplex with two hairpins. This approach was used by Sklenar and Feigon (1990), who demonstrated that such designed oligonucleotides with a loop made of four C's between the purine and the first pyrimidine strands and a loop of three T's between the two pyrimidine strands could, under appropriate conditions, form an intramolecular triplex with seven Watson–Crick and six Hoogsteen base pairs.

We have chosen to use the same approach, but we have replaced the loops made of nucleotide units by a hexaethylene glycol chain. In previous work, we have shown that this type of linker between two complementary DNA strands allows the formation of a duplex with a conformation identical to

0006-2960/92/0431-9197$03.00/0

that of the nonlinked duplex, but with drastically increased stability (Durand et al., 1990). We also showed that this type of hairpin structure maintains its ability to be recognized by proteins (Maurizot et al., 1991). In this work, we present spectrophotometric studies (circular dichroism and UV melting curves) and thermodynamic analyses of the single-stranded oligonucleotide $(dA)_{12}$-x-$(dT)_{12}$-x-$(dT)_{12}$ where x is a hexaethylene glycol chain bridged between the 3′ phosphate of one strand and the 5′ phosphate of the following strand. The data show that this 36-mer oligodeoxynucleotide folds back on itself to form at pH 7 an intrastrand triple helix stabilized by Na^+ or Mg^{2+}. It appears that this intrastrand triplex has the same conformation overall and a higher stability than the interstrand corresponding triplex $(dA)_{12}$·$2(dT)_{12}$. These results show that this single-strand triplex provides a simple model system for studying different effects on the triplex formation such as changes of the sequences in the oligodeoxynucleotide or the interaction with small molecules.

MATERIALS AND METHODS

Oligodeoxynucleotide Synthesis. The synthesis of the 36-mer 5′$(dA)_{12}$-x-$(dT)_{12}$-x-$(dT)_{12}$3′ was achieved on a DNA automatic synthesizer using the phosphoramidite procedure. Introduction of the hexaethyleneglycol linker x was performed following the previously described method (Durand et al., 1990). After unblocking, the 36-mer was purified by liquid chromatography: retention time, 13 min 7 s [Lichrospher RP18 (diameter 5 μm) Merck (125 mm × 4 mm), flow rate 1 mL/min with a linear gradient of acetonitrile from 5% to 80% in a 0.1 M triethylammonium acetate buffer, pH 7].

Solution Preparation. Oligonucleotide solutions were prepared with a buffer containing 10 mM sodium cacodylate and 0.2 mM disodium EDTA, pH 7.0. The desired ionic strength was obtained by additions of either solid or 1 M solution NaCl. The various concentrations of $MgCl_2$ in sample solutions were obtained by additions of concentrated solutions of $MgCl_2$. The concentrations of $(dA)_{12}$-x-$(dT)_{12}$-x-$(dT)_{12}$, $(dA)_{12}$, and $(dT)_{12}$ were determined by UV absorption at 90 °C, i.e., with compounds in the denatured state, assuming as extinction coefficients 8500 and 15000 M^{-1} cm^{-1} for T and A, respectively. The concentration used to calculate the CD amplitude was that of the nucleotide unit. Solutions of $(dA)_{12}$ and $(dT)_{12}$ were combined to give mixtures with a stoichiometric 1:2 ($(dA)_{12}$ to $(dT)_{12}$) molar ratio.

UV Melting Curves. The wavelength dependence of the UV melting profile can give valuable information on the nature of the transition involved in the melting of nucleic acids complexes. Previous studies on the triple-helix formation between poly(dA) and poly(dT) (Riley et al., 1966; Cassani & Bollum, 1969) and between oligodeoxyadenylates and oligothymidilates (Pilch et al., 1990a) showed that the melting of the third strand from the underlying duplex, hereafter referred to as the Hoogsteen (HS) transition, is accompanied by a hyperchromic absorbance change at 284 nm, whereas the denaturation of the duplex strands, hereafter referred to as the Watson–Crick (WC) transition, showed no change. Both of these events, however, are accompanied by hyperchromic absorbance changes at 260 nm. For these reasons, in order to reveal triplex and duplex formation with the 36-mer oligodeoxynucleotide and with the reference mixture $(dA)_{12} + 2(dT)_{12}$, we selected 260 and 284 nm as wavelengths of absorbance measurement versus temperature.

Absorbance versus temperature profiles were measured using an LKB spectrometer interfaced to a microcomputer. The temperature of the cell holder (a four-position rotatable cell turret) was regulated by circulating liquid using a Haake water bath controlled by the microcomputer and measured by a thermistance. A buffer solution of appropriate ionic strength was placed in a reference cuvette occupying one position of the cell turret. Sample solutions were contained in a quartz cuvette with a Teflon stopper. The measurements were initiated at approximately 7 °C, and the temperature was increased up to 95 °C with a 1 °C increment with a 1-min waiting period for stabilization at each temperature. The absorbance data were transferred to a disk for storage and later analyzed. Below 20 °C, nitrogen was continuously flushed through the sample compartment to prevent condensate formation. For comparative visualization purposes, melting profiles are shown with absorbances normalized at 95 °C. Numerical differentiations were performed to obtain differential melting profiles from which melting temperatures (T_m) were deduced.

Circular Dichroism Spectroscopy. Circular dichroism measurements were carried out on a Jobin-Yvon Mark IV dichrograph. Data acquisition and analysis were performed on a computer interfaced to the spectrometer. Optical cells with path lengths of 1.0 cm were used to allow melting curve measurements. The temperature of the cell was adjusted with a circulating refrigerated water bath and held constant to ±0.5 °C. During the experiments, nitrogen was continuously circulated through the cuvette compartment. Dichroism readings were collected at 2 °C intervals in the transition ranges and at 4 °C intervals outside of the transition ranges. Each CD spectrum was run at least twice and checked for possible base-line shifts.

Thermodynamic Analysis of Transition Data. Under the Results section we present evidence that the 36-mer can adopt a triplex form (its denaturation is followed at 284 and 260 nm) and a duplex form (its denaturation is followed at 260 nm). To extract from the melting curves the thermodynamic parameters, enthalpic change (ΔH) and entropic change (ΔS), involved in the formation of the duplex (WC transition) and the triplex (HS transition), we analyzed each transition separately (HS at 284 nm and WC at 260 nm) using a two-state model.

The expression of the extinction coefficient ϵ (in base unit) at the temperature T according to a two-state model is given by

$$\epsilon(T) = \alpha\epsilon_i(T) + (1 - \alpha)\epsilon_f \qquad (1)$$

In this expression, α is the fraction of the 36-mer in either the duplex state for the HG transition or the coil state for the WC transition; ϵ_i is the extinction coefficient for the DNA in either the duplex (HG transition) or the coil state (WC transition); and ϵ_f is the extinction coefficient for the DNA in either the triplex (HG transition) or the duplex state (WC transition).

The extinction coefficients ϵ_i and ϵ_f were assumed to be a linear function of the temperature according to

$$\epsilon_i = aT + b \quad \text{and} \quad \epsilon_f = a'T + b' \qquad (2)$$

The extinction coefficient ϵ_i in the duplex state for the HG transition is the mean value of the two species: the duplex part $(dA)_{12}$-x-$(dT)_{12}$ and the dangling end $(dT)_{12}$ linked to the later.

With the transitions studied (WC and HG) being monomolecular, the molar fraction α is related to the changes in

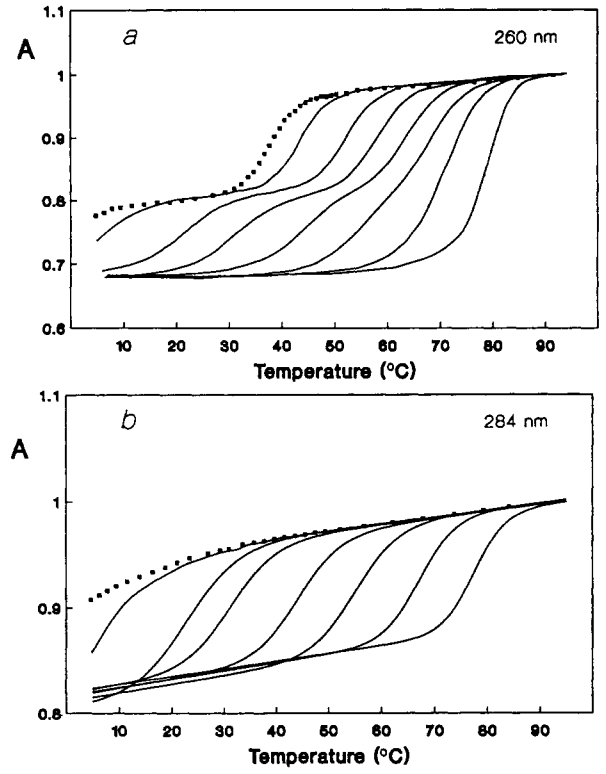

FIGURE 1: Normalized absorbance vs temperature of $(dA)_{12}$-x-$(dT)_{12}$-x-$(dT)_{12}$ for increasing molarities of NaCl (from the left to the right) at 260 nm (a) and 284 nm (b). [NaCl]: 0.00 (□), 0.01, 0.05, 0.10, 0.25, 0.50, 1.00, and 2.00 M.

enthalpy (ΔH) and entropy (ΔS) by the relationship

$$K = \alpha/(1-\alpha) = \exp(-\Delta H/RT + \Delta S/R) \quad (3)$$

Using a nonlinear least-squares method, a program fits experimental melting curves with eq 1, treating ΔH, ΔS, a, b, a', and b' as independent variable parameters. At 260 nm, the domain of fit was limited to the part of the experimental melting curve corresponding to the WC transition.

Salt Dependence of Transition Temperatures. UV melting curves were carried out in the same buffer over a wide range of NaCl concentrations. In the two-state model Δn, the number of ions thermodynamically released per oligomer upon the transition, is given by the relationship

$$\frac{d\,T_m}{d\log[Na^+]} = \left(\frac{2.3RT_m^2}{\Delta H}\right)\Delta n \quad (4)$$

where T_m is the transition midpoint, R is the gas constant, and ΔH is the association enthalpy (Krakauer & Stutervant, 1968; Record et al., 1978; Manning, 1978). Knowing ΔH, Δn can thus be calculated from the salt dependence of T_m.

RESULTS AND DISCUSSION

Effect of NaCl Concentration on the Melting Behavior of the 36-mer. Representative UV melting curves for the 36-mer oligodeoxynucleotide at a concentration of 10^{-4} M (in base unit) are shown at various NaCl concentrations at 260 nm in Figure 1a and at 284 nm in Figure 1b. In the buffer used and without NaCl salt added, the 36-mer shows a one-step melting profile at 260 nm and a monotonic melting profile at 284 nm. The increase of NaCl concentration up to approximately 0.25 M induces a two-step melting profile at 260 nm and a one-step melting profile at 284 nm. The hyperchromicity changes are of 25% and 18% for the first and second step, respectively. The first step at 260 nm corresponds to that found at 284 nm. The sharpness of the transitions observed at 260 nm and 284 nm is indicative of cooperativity. However, we note that at 260 nm the breadth of the first transition is greater than that of the second transition. With NaCl concentrations greater than 0.5 M, the melting profiles at 260 nm become monophasic. For all NaCl concentrations used, we observed no concentration dependence on the melting profiles; this reveals the formation of intramolecular complexes and rules out the possible existence of intermolecular complexes in 36-mer solutions. All subsequent experiments, including CD spectra, were therefore performed at a 10^{-4} M concentration. From these results, and previous studies reported on triplexes containing T·A·T triplets (see Materials and Methods), we deduced that (i) in the absence of NaCl salt the transition observed at 260 nm is a duplex to coil transition, i.e., at the lower temperatures the 36-mer existed in a double-stranded structure with the dangling end x-$(dT)_{12}$; (ii) in the presence of NaCl salt the two transitions observed are the triplex-to-duplex transition followed by the duplex to coil transition, at the lower temperature the 36-mer folded back on itself to adopt a triplex form. In the triplex structure pyr-pur-pyr, it is generally accepted that the third pyrimidine strand is associated with the underlying duplex via Hoogsteen pairing (Rajagopal & Feigon, 1989a; Santos et al., 1989; Stevens & Felsenfeld, 1964; Arnott & Selsing, 1974; Arnott et al., 1974, 1976). NMR studies have recently supported this simple model on the intermolecular triplexes $(dA)_{10}$·$2(dT)_{10}$ (Pilch et al., 1990b) and $(dA)_6$·$2(dT)_6$ (Umemoto et al., 1990). In our experiments, the chemical structure of the 36-mer imposes that the third strand of the triplex is antiparallel to the second one and parallel to the first one.

Table I: T_m Values (°C) for Triplex and Duplex Forms of $(dA)_{12}$-x-$(dT)_{12}$-x-$(dT)_{12}$ in the Presence of NaCl or $MgCl_2$ Salts[a]

[NaCl] (mol/L)	triplex 260 nm	triplex 284 nm	duplex 260 nm
0.00			38.2
0.01			44.0
0.05	21.2	21.7	52.8
0.10	31.0	30.5	58.7
0.25	45.0	45.1	64.4
0.50		56.5	70.1
1.00		67.9	
2.00		78.9	

[$MgCl_2$] (mol/L)	triplex 260 nm	triplex 284 nm	duplex 260 nm
0.000			37.9
0.001	47.0	48.0	59.3
0.002		53.8	
0.004		57.4	
0.010		60.6	
0.020		63.2	
0.100		66.9	

[a] The other experimental conditions were 10 mM sodium cacodylate, 0.2 mM EDTA, pH 7.0. The estimated precision on T_m is ±1 °C.

T_m values, obtained from the method using the derivative of absorbance versus temperature (plots not shown) for all observed transitions at various NaCl concentrations, are listed in Table I. T_m values for the lower temperature transition in biphasic melting curves (260 nm) are essentially identical to T_m values for transitions from the monophasic melting curves (284 nm). For both transitions, the melting temperatures increase with NaCl concentration. Figure 2, which resembles a phase diagram, summarizes the dependence on log [Na^+] of T_m for each of the transitions undergone by the 36-mer.

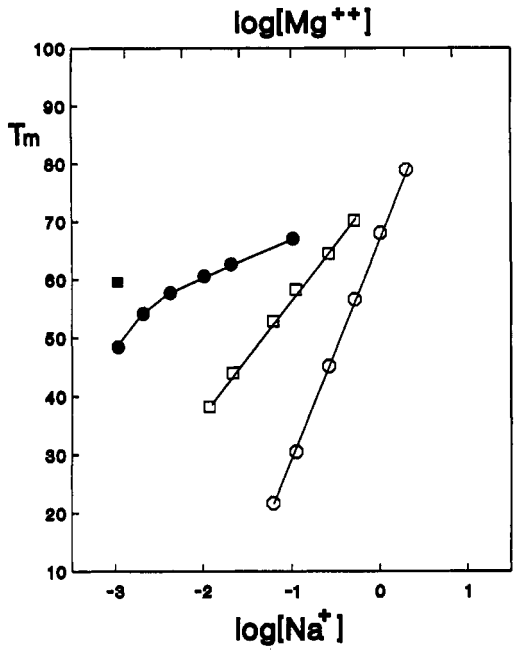

FIGURE 2: Dependence of T_m on log [Na^+] and on log [Mg^{2+}] of transitions undergone by $(dA)_{12}$-x-$(dT)_{12}$-x-$(dT)_{12}$. T_ms in the presence of Na^+ are shown by open symbols; T_ms in the presence of Mg^{2+} are shown by filled symbols: (○) and (●), triplex-to-duplex transition; (□) and (■), duplex-to-coil transition.

For the lower and the upper transition the dependence of the T_m on the concentration of sodium salt is essentially linear with log [Na^+]. Melting temperatures for both, HS and WC, transitions converge as the salt concentration of the sample solution is increased. A 10-fold increase in [Na^+] causes an increase of 36.2 °C in T_m for the triplex-to-duplex transition and an increase of 15.4 °C for the duplex-to-coil transition. Thus, the melting for the triplex-to-duplex transition is considerably more dependent on ionic strength than the melting of the duplex-to-coil transition. In comparison, in 0.01 M sodium phosphate buffer the representations of the T_m of the complexes formed between the homopolymers poly(dA) and poly(dT) exhibit positive slopes of 19 °C for the two-stranded complex and 61 °C for the three-stranded counterpart (Riley et al., 1966). Due to the additional negative charge introduced by the third strand, the charge density of the triplex is greater than that of the duplex. Krakauer and Sturtevant (1968) studying the poly(rA) + poly(rU) system have shown that more Na^+ ions per base pair were bound to the triplex form than to the duplex form. The finding that an increase of the ionic strength raises the T_m value more for the triplex than the duplex form is consistent with the greater charge density of the three-stranded complex. This will be analyzed quantitatively in a following section.

At low ionic strength, the reference mixture $(dA)_{12} + (dT)_{12} + (dT)_{12}$ did not exhibit any transition corresponding either to duplex or triplex formation above 7 °C at a concentration of 10^{-4} M. Figure 3 shows the melting behavior of this reference mixture in 1 M NaCl. It is clear that at the lower experimental temperature (7 °C) the triplex form is not completely promoted. We notice that the breadth of the triplex to duplex transition was greater than that of the corresponding transition in the 36-mer.

Circular Dichroism Studies. CD spectroscopy is highly suitable for distinguishing between different DNA structures. Figure 4 shows the changes in the CD spectra associated with an increasing temperature in the presence of 0.1 M NaCl, a salt concentration which stabilizes below 10 °C the triplex

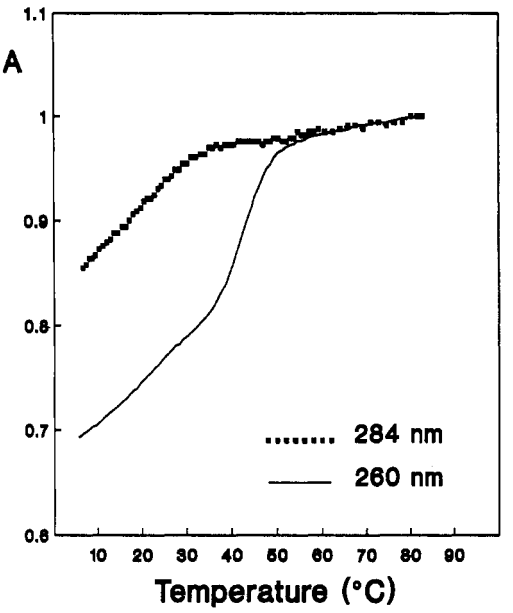

FIGURE 3: Normalized absorbance vs temperature of a $(dA)_{12}$·2-$(dT)_{12}$ solution in the presence of 1 M NaCl at 260 nm and 284 nm.

form of the 36-mer and for which the UV melting profile is distinctly biphasic. To make the figure more legible, we have plotted only selected temperature scans for the Hoogsteen transition (Figure 4a) and for the Watson–Crick transition (Figure 4b).

The melting involves changes in both the amplitude and position of the CD bands. The following observations can be made. (1) The spectrum of the triplex form of the 36-mer is characterized by three maxima at 222, 260, and 281 nm as well as two minima at 248 and 268 nm. (2) The spectrum of the duplex form of the 36-mer is different and characterized by two maxima at 218 and 281 nm and a minimum at 249.5 nm. (3) When the temperature is increased from 1 °C (36-mer in triplex form) to 47 °C (36-mer in duplex form) (Figure 4a), the positive bands at 222 nm and 281 nm show a marked amplitude increase with a slight UV shift for the band at 222 nm, whereas the positive band at 260 nm and the negative band at 248 nm show amplitude decreases and slight red shifts. Two clear isoelliptic points are detected at 265 and 251 nm. (4) When the temperature is increased from 47 °C (36-mer in duplex form) to 90 °C (36-mer in coil form), the positive bands at 218 and 281 nm and the negative band at 249.5 nm show amplitude decreases. Besides, there is a slight red shift for the band at 249 nm and a UV shift for the band at 281 nm. The CD amplitude varies very slightly at 265 nm.

A systematic study of the change of the CD amplitude versus temperature showed that 260 and 251 nm are two convenient wavelengths to follow the HS and WC transitions. Indeed, the denaturation of the duplex is accompanied by an increase at 260 nm and a decrease at 251 nm of the CD amplitude, whereas the transition from the triplex to the duplex form coincides with a decrease of the CD amplitude at 260 nm and a very slight change at 251 nm. The temperature dependences of CD amplitude at 260 and 251 nm in presence of 0.1 M NaCl are shown in Figure 5. We estimate the T_m for the triplex-to-duplex transition equal to 29 °C and the T_m of the duplex-to-coil transition equal to 59 °C or 60 °C (values respectively measured at 251 and 260 nm), whereas those determined by absorption were respectively 30.5 °C and 58.7 °C. Taking into account that the greatest contribution to the uncertainty in T_m comes from the difficulty in locating the limiting temperature dichroism of the triplex, duplex, and

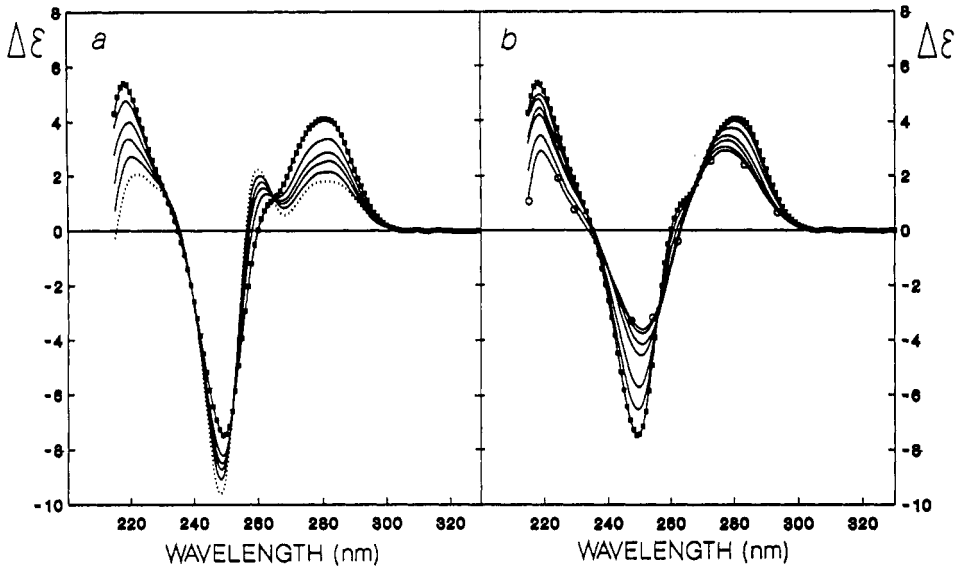

FIGURE 4: CD spectra of $(dA)_{12}$-x-$(dT)_{12}$-x-$(dT)_{12}$ at selected temperatures in the presence of 0.1 M NaCl. (a) Temperatures varying from 1 °C to 47 °C: (···) triple-helix form at 1 °C; (■) double-helix form at 47 °C. (b) Temperatures varying from 47 °C to 90 °C: (■) double helix form at 47 °C; (○) coil form at 90 °C.

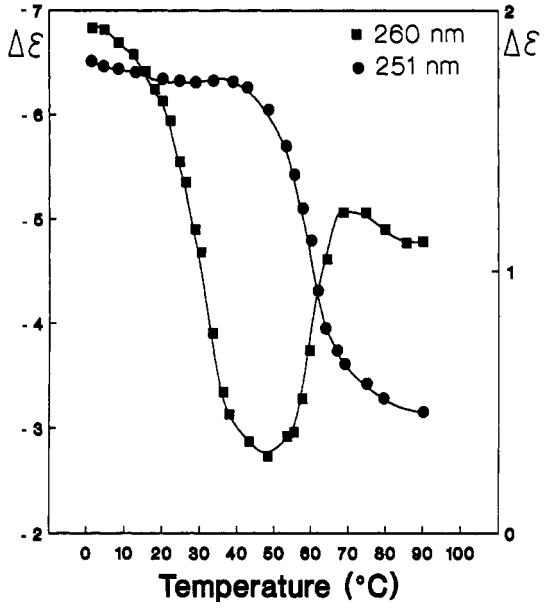

FIGURE 5: CD intensities (Δε) of $(dA)_{12}$-x-$(dT)_{12}$-x-$(dT)_{12}$ at 260 or 251 nm plotted as a function of temperature in the presence of 0.1 M NaCl.

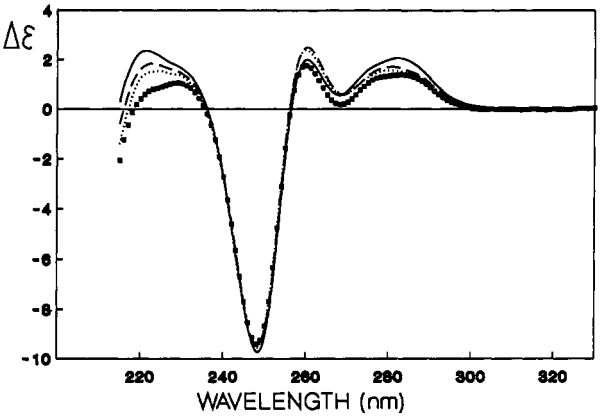

FIGURE 6: Comparison at 1 °C of the CD spectra of $(dA)_{12}$-x-$(dT)_{12}$-x-$(dT)_{12}$ and the reference mixture $(dA)_{12}$ + $(dT)_{12}$ + $(dT)_{12}$: $(dA)_{12}$-x-$(dT)_{12}$-x-$(dT)_{12}$ in the presence of either 1 M NaCl (- - -) or 20 mM $MgCl_2$ (···); $(dA)_{12}$ + $(dT)_{12}$ + $(dT)_{12}$ in the presence of either 1 M NaCl (—) or 50 mM $MgCl_2$ (■).

coil forms of the 36-mer, we conclude that the T_m values respectively determined from CD spectroscopy and absorption UV spectroscopy are in agreement.

At 1 °C and in 1 M NaCl, the salt concentration at which we observed a slight denaturation of its triplex form, the reference mixture $(dA)_{12}$ + $(dT)_{12}$ + $(dT)_{12}$ exhibits nevertheless a spectrum with a shape which is qualitatively similar to that of the 36-mer triplex (Figure 6). The differences observed are essentially in the intensity of the bands. Relative to the 36-mer triplex, we remark that the band centered at 222 nm is slightly more intense, whereas the band centered at 265 nm is slightly less intense. It is noteworthy that the same type of CD variation was observed during the denaturation of the 36-mer triplex and therefore reflects only the fact that the reference mixture is not fully in triple-stranded structure as shown in Figure 3.

Effect of $MgCl_2$ Concentration on the Melting Behavior of the 36-mer. Mg^{2+} has been very often used to promote the formation of triple-stranded structure; we therefore decided to investigate the effect of this divalent cation on our system. Representative UV melting curves for the 36-mer at various $MgCl_2$ concentrations from 1 mM to 100 mM are shown in Figure 6. The thermal denaturation of the 36-mer is accompanied by a hyperchromic effect both at 260 nm (Figure 7a) and at 284 nm (Figure 7b). In the presence of the lower $MgCl_2$ concentration added (1 mM), the profile is slightly biphasic at 260 nm (Figure 7a). From the first-derivative plot (data not shown), the biphasic nature of the melting profile is clearer with a T_m value of 47 °C for the first transition and 59.3 °C for the second transition. The single transition observed at 284 nm presents a T_m of 48 °C. Therefore, the lower T_m corresponds to the triplex-to-duplex transition whereas the higher T_m corresponds to the duplex-to-coil transition. The biphasic aspect of the melting profiles at 260 nm disappears as the $MgCl_2$ concentration increases. Hence, it was not possible to determine the T_m values for the duplex-to-coil transition at an $MgCl_2$ concentration higher than 1 mM. T_m values obtained at 284 nm for the triplex denaturation are listed in Table I. A representation of the T_m of the triplex at different Mg^{2+} ion concentrations is given in Figure 2. The T_m dependence on the concentration of $MgCl_2$ is linear with

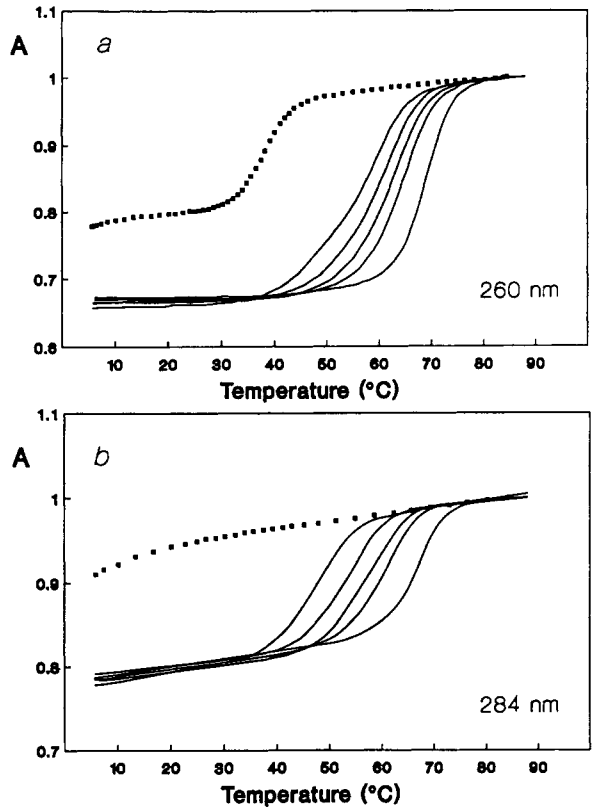

FIGURE 7: Normalized absorbance vs temperature of $(dA)_{12}$-x-$(dT)_{12}$-x-$(dT)_{12}$ for increasing molarities of $MgCl_2$ (from the left to the right) at 260 nm (a) and 284 nm (b). [$MgCl_2$]: 0.000 (■), 0.001, 0.002, 0.004, 0.010, and 0.100 M.

log [Mg^{2+}] for concentrations of $MgCl_2$ larger than 4 mM. As expected according to the Manning theory (Manning, 1978) in the salt concentration range used in this study, the Mg^{2+} ions stabilize the triplex 36-mer much more than the Na^+ ions. So, at 0.1 M salt concentration the T_ms of the triplex denaturation measured at 284 nm are equal to 66.9 °C with $MgCl_2$ and 30.5 °C with NaCl. Furthermore, the slope of the linear dependence of the T_m versus log [Mg^{2+}] is less sharp than the corresponding slope in the presence of NaCl salt. For the triplex denaturation, a 10-fold increase in salt concentration cause a rise of 7 °C with $MgCl_2$ and 36.2 °C with NaCl.

No significant change was noticed in the shape of the CD spectra as the $MgCl_2$ concentration increased from 0 to 100 mM (data not shown). The CD spectrum of the triplex measured at 1 °C in the presence of 20 mM $MgCl_2$ and that of the triplex in the presence of 1 M NaCl salt are presented in Figure 6. They are very similar. Hence, the conformation of the triplex formed with the 36-mer is not dependent on the type of cationic environment, monovalent Na^+ or divalent Mg^{2+}, and for both ions it does not depend on the concentration of salt in the range studied.

The UV melting profile of the reference mixture $(dA)_{12}$ + $(dT)_{12}$ + $(dT)_{12}$ in the presence of 50 mM $MgCl_2$ demonstrated that this mixture was in triplex form (data not shown). However, the intensity of the CD spectrum of the 36-mer triplex obtained in the presence of 20 mM $MgCl_2$ is slightly different from the intensity of the spectrum of the triplex form of the reference mxiture $(dA)_{12}$ + $(dT)_{12}$ + $(dT)_{12}$ obtained in the presence of 50 mM $MgCl_2$ (Figure 6). This reflects a small difference between the structures of the intra- and intermolecular complexes due to a difference of binding Mg^{2+}; this difference might be due to end effects resulting from the hexaethylene glycol chains. Nevertheless, taking into consideration that all spectra shown in Figure 6 present a great similarity and that the 36-mer triplex spectra are also qualitatively similar to that described for analog sequences as $(dA)_{10}$·$(dT)_{10}$·$(dT)_{10}$ (Pilch et al., 1990a,b), we conclude that the intrastrand triplex formed with the modified single-strand 36-mer has a conformation close to that formed with the complementary single strand $(dA)_{12}$ and $(dT)_{12}$.

Table II: Thermodynamic Parameters[a] of $(dA)_{12}$-x-$(dT)_{12}$-x-$(dT)_{12}$

[NaCl] (mol/L)	Hoogsteen interaction			Watson–Crick interaction		
	T_m (°C)	$-\Delta H$	$-\Delta S$	T_m (°C)	$-\Delta H$	$-\Delta S$
0.00				38.1	72.5	233
0.01				43.9	75.5	238
0.05	22.2	35.8	121	52.6	73.2	225
0.10	31.4	41.9	138	58.2	70.5	213
0.25	44.4	48.9	154	63.9	69.9	207

[a] The enthalpic and entropic variations are respectively expressed in kilocalories per mole and calories per mole per degree. Mole refers to a mole of the structure formed (duplex for WC interaction or triplex for HS interaction). The estimated precision on ΔH and ΔS is ±10%.

Thermodynamic Analysis of the UV Melting Curves. In the presence of NaCl salt, the isoelliptic points apparent in the temperature-dependent CD spectra suggest a two-state event for the denaturation of the 36-mer, for both transitions (Figure 4a,b). In the presence of the $MgCl_2$ concentration used and for NaCl concentrations larger than 0.25 M, we could not afford to observe clearly isoelliptic points because of the proximity of the two transitions. This proximity does not allow a comparison of the thermodynamic parameters of the coil-to-duplex transition with those of the duplex-to-triplex transition in this salt.

Thermodynamic parameters obtained from analysis previously exposed in the Materials and Methods section are listed in Table II. Some striking facts emerge from the values in the Table II. For both transitions (WC or HS), the thermodynamic parameters exhibit a variation with the salt concentration. However, the variations observed for the two transitions are drastically different. In the case of the WC transition, we observe a small decrease, by about 10%, of the value of $-\Delta H$ and $-\Delta S$ when the salt is increased from 0 to 0.25 M NaCl. This small variation is very near the limit of the precision of our analysis; nevertheless we feel that it corresponds to a reality since the variation was regular (see Table I) and was obtained for several series of experiments. On the contrary, the variation of the thermodynamic parameters corresponding to the HS transition corresponds to an increase of $-\Delta H$ and $-\Delta S$ with the salt concentration. The increase of these parameters is approximately 30% when the concentration of NaCl increases in the same range (0–0.25 M).

The shape of the melting profiles allowed determination of the parameters for both (HS and WC) transitions only with an NaCl concentration from 0.05 M to 0.25 M, where the curves are clearly biphasic. In this range of salt concentration, it appears that in the triplex the HS part is enthalpically more stable but entropically less stable than the WC part. For instance, in 0.1 M NaCl, ΔH = –41.9 kcal/mol and ΔS = –138 eu for the HS transition whereas ΔH = –70.5 kcal/mol and ΔS = –213 eu for the WC transition. This difference of stability between the HS part and the WC part of the triplex is salt concentration-dependent, decreasing as the NaCl concentration increases (Table II).

The factors which contribute to the stability of ordered oligonucleotide structures in solution are numerous: (i) hydrogen bonding and stacking interaction between bases; (ii) interactions arising from the charges of the phosphate

Table III: Counterion Release in the Transitions of $(dA)_{12}$-x-$(dT)_{12}$-x-$(dT)_{12}$[a]

	d T_m/(d log [Na^+]) (K)	$RT_m^2/\Delta H$ (K/mol)	Δn
Hoogsteen transition	36.2 ± 0.5	4.5 ± 0.4	3.5 ± 0.3
Watson–Crick transition	15.4 ± 0.5	2.9 ± 0.3	2.3 ± 0.3

[a] The slopes of the T_m vs log [Na^+] plots were obtained by least-squares analysis. The values of $RT_m^2/\Delta H$ represent the average determination in several salt buffer solutions.

groups, comprising the electrostatic interaction between the charged phosphate groups themselves, but also the interaction of the phosphate groups with the ions in the surrounding solution; (iii) end effects. That the enthalpy change was less negative for the HS interaction than that for WC interaction matches the observed reduction in stability of HS relative to the corresponding WC interaction. This can be attributed to the fact that in the triplex the opposite phosphate groups in the two parallel chains in the HS part are in closer proximity than those in the WC part and consequently induce higher phosphate–phosphate electrostatic repulsions. This is consistent with a lower T_m value for the triplex than for the duplex form. As the salt concentration increases, the repulsions of the phosphate groups decrease due to the more effective screening, so that the stability of the HS part is closer and closer to that of the WC part, as this is reflected by the apparent monophasic aspect of the UV melting profiles measured at 260 nm and at the highest salt concentrations used. In contrast, the decrease of the entropic barrier for the Hoogsteen interaction relative to the WC interaction can be in part attributed to the solvent effects. Positive entropy change is associated with the removal of water from apolar residues. It is possible that there are more water molecules freed upon the triplex formation than upon the duplex formation.

The less negative ΔH and ΔS values of HS interactions relative to those of WC interactions match previous studies on the formation of DNA triplexes by short oligonucleotides (Pilch et al., 1990a,b; Xodo et al., 1990; Manzini et al., 1990) or by a mixture of poly(rA) and poly(rU) (Krakauer & Sturtevant, 1968).

Considering that the 36-mer triplex is made up of 12 T·A·T triplets, it follows that each pyrimidine residue binding in the major groove of the duplex is accompanied by a mean enthalpy change of −3.5 kcal/mol. Xodo et al. (1990), with a DNA triplex containing a loop and comprising a stem with 6 T·A·T triplets and 4 C^+·G·C triplets, reported an enthalpy change (less the protonation) for each pyrimidine binding into the major groove of −5.8 kcal/mol. Manzini et al. (1990); with a DNA triplex containing a hairpin and a stem comprising 5 T·A·T triplets and 6 C^+·G·C triplets, reported for each HS pairing a value of −6.6 kcal/mol. These differences may arise from variations in the base composition, concentrations, type of cations, and pH. However, our values are higher than those reported by Pilch et al. (1990a,b) for the intermolecular triplex $(dA)_{10}$·$2(dT)_{10}$. They determined, in the presence of 50 mM $MgCl_2$, 10 mM sodium cacodylate, and 0.1 mM EDTA and at pH 5.5, an enthalpy change of −2.3 kcal/mol occurring upon the formation of the HS part of the triplet. It should be noticed that with the same analysis of the UV melting profiles as those of Pilch et al. (1990a,b), in a similar buffer, but with 20 mM $MgCl_2$ and at pH 7, we obtained for HS base pair formation an enthalpy change of −3.9 kcal/mol with the reference intermolecular triplex $(dA)_{12}$·$2(dT)_{12}$.

From the thermodynamic data given in Table II and from the slope of the T_m vs log [Na^+] (Figure 2), one can estimate the amount of sodium ions, Δn, which are thermodynamically released in the HS and in the WC transitions. These values are given in Table III. They are related to the number of ions thermodynamically bound per phosphate in the triplex, duplex, and coil forms (respectively, i_T, i_D, i_C). For the HS transition

$$36i_T \rightarrow 24i_D + 12i_C$$

therefore

$$\Delta n(\mathrm{HS}) = 36i_T - 24i_D - 12i_C \quad (5)$$

Whereas for the WC transition

$$24i_D + 12i_C \rightarrow 36i_C$$

it follows that

$$\Delta n(\mathrm{WC}) = 24i_D - 24i_C \quad (6)$$

From these two equations, one can calculate the Δi(HS) and Δi(WC) which are the variations per phosphate associated with each transition. We found a value of $\Delta i(\mathrm{WC}) = \Delta n(\mathrm{WC})/24 = 0.096$. For comparison, a value of 0.17 was determined from the melting of polymeric DNA. On an octamer, Erie et al. (1987) found a value of 0.096 whereas Braunlin and Bloomfield (1991) reported a value of 0.13. Park and Breslauer reported a value of 0.13 for two decamers. Record and Lohman (1978) have derived a semiempirical theory of the electrostatic end effect and calibrated it with the hairpin data of Elson (1970). For duplex dissociation to single strands they tentatively predicted

$$\Delta i_N = \Delta i_\infty(1 - 7.94/N)$$

where N is the number of phosphates in the oligomer duplex.

In our system, we can assume that the linker is long enough to enable the phosphate of the dangling $(dT)_{12}$ arm to have no influence on the duplex part of the oligomer. The theory therefore predicts that for the WC transition the value of Δi should be $0.17 \times 0.67 = 0.11$ in agreement with the experimental result.

For the HS transition combining eqs 5 and 6, we found a value of $\Delta i(\mathrm{HS}) = i_T - i_D = 0.065$. To our knowledge, these are the first data on a triplex oligonucleotide. This is no doubt due to the difficulty in obtaining a stable structure as previously mentioned. For long polymeric poly(A)·2(poly(U)), the corresponding Δi is equal to $0.93 - 0.89 = 0.04$ according to the data reported by Record et al. (1978). One must be cautious before drawing conclusions from the comparison between this value and that we have found since, as for the duplex-to-coil transition, one can expect an effect on the length of the oligomer. Nevertheless, it is interesting to notice that the Δi between the triplex and the duplex is smaller than that found between the duplex and the coil. It certainly would be of interest to perform theoretical calculations on the oligoelectrolyte end effect for the triplex structure as previously made on the duplex either by a semiempirical approach (Record & Lohman, 1978) or by a Grand Canonical Monte Carlo analysis (Olmsted et al., 1989, 1991).

CONCLUSION

We have reported experimental evidence that, in appropriate salt conditions, the 36-mer modified oligonucleotide $(dA)_{12}$-x-$(dT)_{12}$-x-$(dT)_{12}$, where x is a hexaethylene glycol chain, folds back twice on itself to form an intramolecular triplex whose conformation is close to that of the reference triplex

$(dA)_{12}$·2$(dT)_{12}$. Whatever the type of salt NaCl or $MgCl_2$, the intramolecular triplex is more stable than the reference intermolecular triplex. Magnesium chloride facilitates intramolecular triplex formation more than the sodium chloride. However, it is noteworthy that the divalent cation Mg^{2+} is not required for the intramolecular triplex formation as it is most of the time when an intermolecular triplex is formed with short oligonucleotides. The stability of the Hoogsteen part of the intramolecular triplex studied in this work is generally weaker than the Watson–Crick part. The stability of the triplex is more ionic strength dependent than the stability of the underlying duplex.

To summarize, our results show that, compared to those of the intermolecular triplex formation, the experimental conditions in the formation of an intramolecular triple-helical DNA of pyr-pur-pyr are less restricting; consequently a shorter triplex stem can be formed in a much lower DNA concentration. We think that this model of an oligomer triplex, rather than the reference intermolecular triplex, provides an opportunity to study under easier experimental conditions the properties of these helices such as, for example, the interaction of small molecules such as intercalators. In this perspective, additional studies on defined helices formed on the base of the model will be carried out.

REFERENCES

Antao, V. P., Gray, D. M., & Ratliff, R. L. (1988) *Nucleic Acids Res. 16*, 719–739.

Arnott, S., & Selsing, E. (1974) *J. Mol. Biol. 88*, 509–521.

Arnott, S., Chandrasekaran, R., Hukins, D. W. L., Smith, P. J. C., & Watts, L. (1974) *J. Mol. Biol. 88*, 523–533.

Arnott, S., Bond, P. J., Selsing, E., & Smith, P. J. C. (1976) *Nucleic Acids Res. 3*, 2459–2470.

Braulin, W. H., & Bloomfield, V. A. (1991) *Biochemistry 30*, 754–758.

Cassani, G. R., & Bollum, F. J. (1969) *Biochemistry 8*, 3928–3936.

Cooney, M., Czernuszewicz, G., Postel, E. H., Flint, S. J., & Hogan, M. E. (1988) *Science 241*, 456–459.

Douglas, J. S., Johnson, D. A., & Morgan, A. R. (1979) *Nucleic Acids Res. 6*, 3073–3091.

Durand, M., Chevrie, K., Chassignol, M., Thuong, N. T., & Maurizot, J. C. (1990) *Nucleic Acids Res. 18*, 6353–6359.

Elson, E. L., Scheffler, I. E., & Baldwin, R. L. (1970) *J. Mol. Biol. 54*, 401–415.

Erie, D., Sinha, N., Olson, W., Jones, R., & Breslauer, K. (1987) *Biochemistry 26*, 7150–7165.

Federova, O. S., Knorre, D. G., Podust, L. M., & Zarytova, V. F. (1988) *FEBS Lett. 228*, 273–276.

Felsenfeld, G., Davies, D. R., & Rich, A. (1957) *J. Am. Chem. Soc. 79*, 2023–2024.

Francois, J. C., Saison-Behmoras, T., & Helene, C. (1988) *Nucleic Acids Res. 16*, 11431–11440.

Francois, J. C., Saison-Behmoras, T., Thuong, N. T., & Helene, C. (1989) *Biochemistry 28*, 9617–9619.

Hanvey, J. C., Shimizu, M., & Wells, R. D. (1988) *Proc. Natl. Acad. Sci. U.S.A. 85*, 6292–6296.

Htun, H., & Dahlberg, E. (1988) *Science 241*, 1791–1796.

Johnson, B. H. (1988) *Science 241*, 1800–1804.

Kibler-Herzog, L., Kell, B., Zon, G., Shinozuka, K., Mizan, S., & Wilson, W. D. (1990) *Nucleic Acids Res. 18*, 3545–3555.

Kohwi, Y., & Kohwi-Shigematsu, T. (1988) *Proc. Natl. Acad. Sci. U.S.A. 85*, 3781–3785.

Krakauer, H., & Sturtevant, J. M. (1968) *Biopolymers 6*, 491–512.

Le Doan, T., Perrouault, L., Praseuth, D., Habhoub, N., Decout, J. L., Thuong, N. T., Lhomme, J., & Hélène, C. (1987) *Nucleic Acids Res. 15*, 7749–7760.

Lee, J. S., Burkholder, G. D., Latimer, L. J. P., Haug, B. L., & Braun, R. P. (1987) *Nucleic Acids Res. 15*, 1047–1061.

Lyamichev, V. I., Mirkin, S. M., & Frank-Kamenetskii, M. D. (1986) *J. Biomol. Struct. Dyn. 3*, 667–669.

Lyamichev, V. I., Mirkin, S. M., & Frank-Kamenetskii, M. D., & Cantor, C. R. (1988) *Nucleic Acids Res. 16*, 2165–2178.

Manning, G. S. (1978) *Q. Rev. Biophys. 11*, 179–246.

Manzini, G., Xodo, L. E., Gasparotto, D., Quadrifoglio, F., van der Marel, G. A., & van Boom, J. H. (1990) *J. Mol. Biol. 213*, 833–843.

Marck, C., & Thiele, D. (1978) *Nucleic Acids Res. 5*, 1017–1028.

Maurizot, J. C., Chevrie, K., Durand, M., & Thuong, N. T. (1991) *FEBS Lett. 288*, 101–104.

Michelson, A. M., Massoulie, J., & Gushchelbauer, W. (1967) *Prog. Nucleic Acid Res. Mol. Biol. 6*, 83–141.

Mirkin, S. M., Lyamichev, V. I., Drushlyak, K. N., Dobrynin, V. N., Filippov, S. A., & Frank-Kamenetskii, M. D. (1987) *Nature 330*, 495–497.

Morgan, A. R., & Wells, R. D. (1968) *J. Mol. Biol. 37*, 63–80.

Moser, H. E., & Dervan, P. B. (1987) *Science 238*, 645–650.

Olmsted, M. C., Anderson, C. F., & Record, M. T. (1989) *Proc. Natl. Acad. Sci. U.S.A. 86*, 7766–7770.

Olmsted, M. C., Anderson, C. F., & Record, M. T. (1991) *Biopolymers 31*, 1593–1604.

Park, Y. W., & Breslauer, K. J. (1991) *Proc. Natl. Acad. Sci. U.S.A. 88*, 1551–1555.

Perrouault, L., Asseline, U., Rivalle, C., Thuong, N. T., Bisagni, E., Giovannangeli, C., Le Doan, T., & Hélène, C. (1990) *Nature 344*, 358–360.

Pilch, D. S., Brousseau, R., & Shafer, R. H. (1990a) *Nucleic Acids Res. 18*, 5743–5750.

Pilch, D. S., Levenson, C., & Shafer, R. H. (1990b) *Proc. Natl. Acad. Sci. U.S.A. 87*, 1942–1946.

Posvic, T., & Dervan, P. (1989) *J. Am. Chem. Soc. 111*, 3059–3062.

Praseuth, D., Perrouault, L., Le Doan, T., Chassignol, M., Thuong, N. T., & Hélène, C. (1988) *Proc. Natl. Acad. Sci. U.S.A. 85*, 1349–1353.

Rajagopal, P., & Feigon, J. (1989a) *Nature 339*, 637–640.

Rajagopal, P., & Feigon, J. (1989b) *Biochemistry 28*, 7859–7870.

Record, M. T., & Lohman, T. (1978) *Biopolymers 17*, 159–166.

Record, M. T., Anderson, C. G., & Lohman, T. (1978) *Q. Rev. Biophys. 11*, 103–178.

Riley, M., Mailing, B., & Chamberlin, M. J. (1966) *J. Mol. Biol. 20*, 359–389.

Santos, C. D. L., Rosen, M., & Patel, D. (1989) *Biochemistry 28*, 7282–7289.

Sklenar, V., & Feigon, J. (1990) *Nature 345*, 835–838.

Stevens, C. L., & Felsenfeld, G. (1964) *Biopolymers 2*, 293–314.

Strobel, S. A., Moser, H. E., & Dervan, P. B. (1988) *J. Am. Chem. Soc. 110*, 7927–7929.

Umemoto, K., Sarma, M. H., Gupta, G., Luo, J., & Sarma, R. H. (1990) *J. Am. Chem. Soc. 112*, 4539–4545.

Voloshin, O. N., Mirkin, S. M., Lyamichev, V. I., Belotserkovskii, B. P., & Frank-Kamenetskii, M. D. (1988) *Nature 333*, 475–476.

Wells, R. D., Collier, D. A., Hanvey, J. C., Shimizu, M., & Wohlrab, F. (1988) *FASEB J. 2*, 2939–2949.

Xodo, L. E., Manzini, G., & Quadrifolglio, F. (1990) *Nucleic Acids Res. 12*, 3557–3564.